

BEAM HALO MONITORING AT CTF3

T. Lefèvre, Northwestern University, Evanston, USA

H. Braun, E. Bravin, R. Corsini, D. Schulte and A.L. Perrot, CERN, Geneva, Switzerland

Abstract

In high intensity accelerators, the knowledge of the beam halo distribution and its generation mechanisms are important issues. In order to study these phenomena, dedicated beam diagnostics must be foreseen. In circular machines, beam halo is monitored by using scrapers and beam loss detectors. In the framework of the CLIC project, a beam halo monitor is currently under development. The proposed device is based on an imaging system and a masking technique, which suppresses the core of the beam to allow direct observation of the halo. A first test was performed on the CLIC Test Facility 3 in 2003. We discuss the performances and the limitations of this technique pointing out our plans for future developments.

1 INTRODUCTION

An analogy can be made between beam halo monitoring and the detection of faint emissions very close to much brighter objects in Astronomy. Astrophysicists have been developing the Coronagraph [1] [2], which is a telescope using two consecutive masks which remove the central part of an initial image which thus allow the detection of off axis light sources with a high dynamic range.

With the development of high intensity accelerators [3], physicists are more and more demanding in terms of beam diagnostic accuracy and performances. The dynamic range of any device must be increased to guarantee the normal behaviour of the beam. State of the art cameras can propose a 90dB dynamic range measurement [4] but are at the moment very expensive. This makes their use not compatible with the radioactive environment of an accelerator. One can think of using an optical line to bring the photons in a separate room where the camera can be operated safely. But in this case, aberrations in the optical line may alter the accuracy of the measurement. 8 to 10bits CCD cameras are classically used in accelerators but limit the detection to a 40-60dB dynamic range. For the measurement of the beam halo distribution the dynamic range must be increased by at least a few orders of magnitude (>80dB).

We present in this paper a method for beam halo reconstruction using an Optical Transition Radiation (OTR) screen and an optical masking technique. The results of a preliminary test performed on the CLIC Test Facility 3 [3], with 35MeV electrons are presented. The goal of this test was to check the performances and the limitations of the present set-up. Some possible improvements are finally suggested.

2 OPTICAL SET-UP

The optical set-up is composed of two parts. A set of two achromatic lenses focus the light emitted by the electrons on a first image plane where a mask, consisting of a spot printed on a polyester foil, sits. A second set of lenses reimage the mask on a CCD camera. The light intensity can be adjusted remotely controlled by rotating a filter wheel located just before the first image plane. The different filters provide a fixed attenuation of 2, 10, 100 and 1000. The mask is installed on a remotely controlled translation stage so that its position can be modified to follow the beam position with $1\mu\text{m}$ step resolution. Only a few patterns are available on the polyester foil and therefore in this test the electron beam size was adjusted to the mask size. A picture of the optical system is shown in Figure 1.

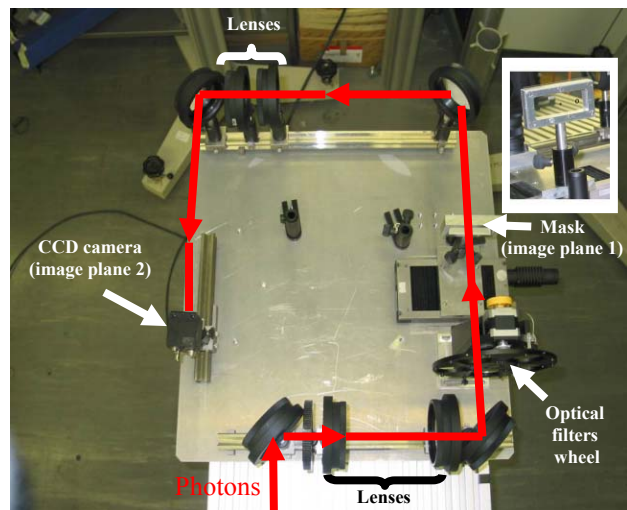


Figure 1: Optical set-up of the beam halo imager

The focal length of the lenses are chosen to fit the experimental constraint. The overall optical magnification is 0.1 in order to view on the CCD the total surface of the OTR screen ($\varnothing 35\text{mm}$). With 35MeV electrons, the OTR angular distribution is large and we considered that most of the emitted photons are contained in a $5/\gamma$ cone angle (with γ the relativistic factor). To collect as much light as possible, the distance between the screen and the first lens is set to a minimum value of 70cm, limited by the vacuum tank design. A calibration of the mask opacity has been realized in our optical lab. A calibration plate, consisting of a central big hole and smaller off axis holes, is simulating the core of the beam and its halo. By

moving the mask in and out of the central hole, one can measure the performances of our system. Two pictures, with and without the mask as acquired are shown on Figure 2. A 1% transmission optical density filter is placed just in front of the camera. The two images are then analyzed taking a horizontal projection of the light intensity inside the red area visible in Figure 2a and 2b.

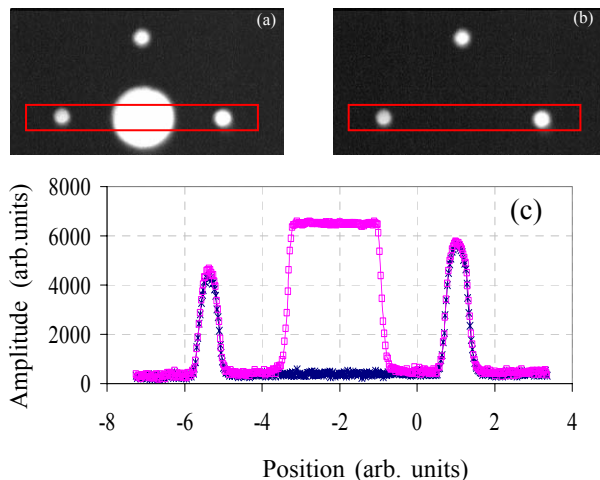


Figure 2: Results of the calibration test: Two pictures showing the calibration plate without (a) and with (b) the mask. (c) analysis of the two images

The difference in amplitude visible in Figure 2(c) between the central part and the smaller holes comes from a non homogeneous illumination of the calibration plate. Optical simulations have been done using ZEMAX [5] to check the light transmission of OTR light for off-axis particles. The relative illumination of the CCD is constant all over the screen size as shown on Figure 3.

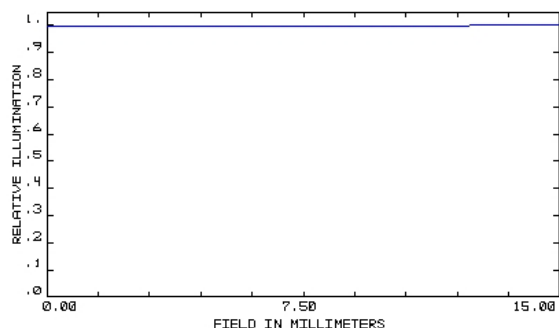


Figure 3: CCD illumination simulated with ZEMAX

The point spread function for an on-axis particle is $18\mu\text{m}$ r.m.s and increases because of aberrations up to $35\mu\text{m}$ for far off-axis particles. With expected beam spot sizes around 1mm , this is not a issue for our test.

From the images on Figure 2(b), the mask opacity is measured by removing the optical density filter placed in front of the camera. The result is shown in Figure 4 and the mask opacity is better than 10^3 .

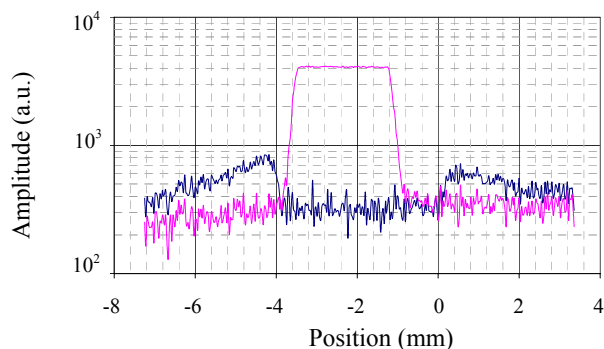


Figure 4: Measurement of the mask opacity

3 BEAM HALO IMAGES

For beam halo imaging, it is important to use a photon source with intensities linearly proportional to the beam charge. Optical Transition Radiators provide a very reliable source with a total number of photons per electron in the wavelength range $[\lambda_a, \lambda_b]$ given by [6]:

$$N_{OTR} = \frac{2\alpha R}{\pi} \left[\left(\beta + \frac{1}{\beta} \right) \cdot \ln \left(\frac{1+\beta}{1-\beta} \right) - 2 \right] \ln \left(\frac{\lambda_b}{\lambda_a} \right)$$

with α the fine structure constant, β the electrons velocity, γ the electrons relativistic factor and R the reflectivity of the OTR screen.

The measurements have been performed on the CTF3 linac using a $10\mu\text{m}$ Al OTR screen and 35MeV electrons. $8.4 \cdot 10^{-23}$ photons per electron are emitted from the screen in the $[400, 600]\text{nm}$ wavelength range.

Some examples of the acquired images are given in Figure 5. Column (a) shows images of the beam measured without the mask and with a 10% optical density filter. This corresponds to classical beam imaging conditions. Column (b) shows images with the mask centred on the beam core. Column (c) represents images of the beam halo measured when removing the optical density filter.

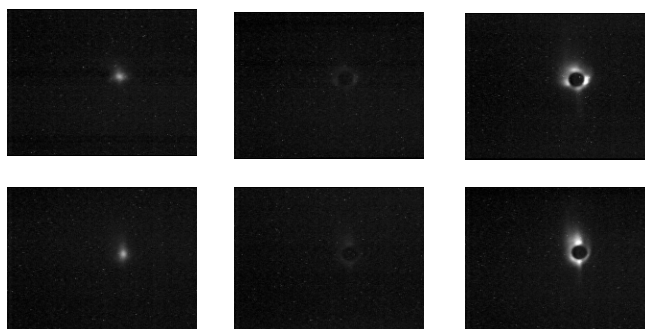


Figure 5: Images of beam halo measurements.

From the images (a), (b) and (c), a higher dynamic range beam image is reconstructed using the following analysis. The beam core is isolated by subtracting image (b) from image (a). The corresponding pixel values are multiplied by a factor equivalent to the filter density difference between images (a) and (c). In our case, this corresponds to a factor 10. This new image is finally

superimposed with the one from column (c). A comparison between the beam image obtained using a classical imaging system (a) and the beam halo method (b) are given in Figure 6.

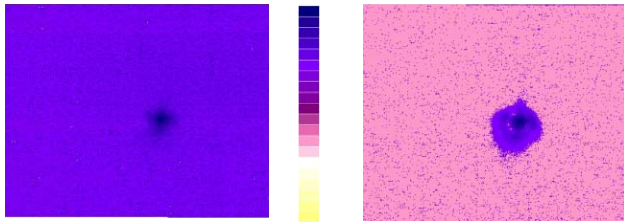


Figure 6: Comparison between a normal CCD camera measurement (a) and the beam halo reconstruction (b).

The images on Figure 6 are represented with a logarithmic scale. In the case of images (a) and (b), the mask fits correctly the beam shape and the masking technique offers a 10 times better dynamic range. The vertical profiles extracted from the images (a) and (b) are shown in Figure 7. The curves are fitted using a Gaussian distribution and the r.m.s. beam size measured from image (b) gives a value 9% smaller compared to the one from image (a). The shape of the beam transverse distribution can be also resolved with better accuracy, showing for example here that the beam profile is not perfectly Gaussian, but show a small pedestal which was not observable via a classical measurement.

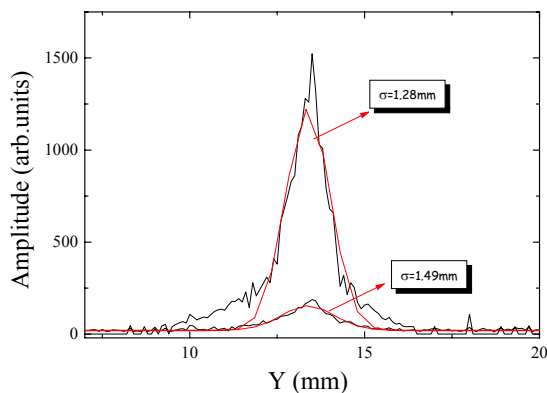


Figure 7: Example of a vertical profile measurement

4 PERSPECTIVES & LIMITATIONS

A first test of beam halo monitoring has been done on the CLIC Test Facility 3. The light emitted from an OTR screen is imaged on a CCD camera. A mask placed at a first image plane is used to suppress the core of the beam and the beam halo was thus observed by removing optical densities. In these conditions, the dynamic range of our beam imaging system has been improved by a factor 10.

In this test the main limitation comes from the fact that the OTR light intensity was not intense enough to explore further the halo distribution. An easy way to improve our set-up would be to use an intensified camera.

However even if we supposed that the available light intensity is not limited, the masking technique must follow the beam halo size as far as it is observed to avoid the saturation of the camera. Adaptive optics can provide a way of adjusting the beam image size to the mask size by changing the focal length of the optical system. This can be done for example by moving back and forth a lens but the shape of the mask is still not modified.

To provide an efficient device, more sophisticated masking techniques must be developed to fit the mask size automatically to the beam size. An alternative would be to use a programmable mask which can follow the beam size. Technical solutions exist either based on micro mirror array [7] or liquid crystal devices, but are relatively expensive and not radiation resistant.

On CTF3 and CLIC, with the long pulse train, it can be very useful to have a gated camera which provides the time evolution of the beam size and allows the time dependent study of the beam halo mechanism. State of the art gated cameras can have gating times down to 50ps [8].

5 ACKNOWLEDGMENT

This research was partially supported by the Illinois Consortium for Accelerator Research, agreement number ~228-1001.

6 REFERENCES

- [1] B. Lyot, MNRAS, 99, (1939)
- [2] M.J. Kuchner and D.N. Spergel, Astrophysics Journal, 594, 617, (2003).
- [3] R. Corsini et al, "First Full Beam Loading Operation with the CTF3 Linac", these conference.
- [4] Deep Cooled Digital camera, model ORCA-AG: <http://usa.hamamatsu.com/en/products/system-division/cameras/high-sensitivity/>
- [5] ZEMAX software: <http://www.zemax.com/>
- [6] L. Wartski, Thesis, Orsay, (1976).
- [7] Accessory Light Modulator Package by VIALUX: <http://www.vialux.de>
- [8] Standard Gated Optical Imager by Kentech Instruments: <http://www.kentech.co.uk/imagers.html>